Hindawi Publishing Corporation
The Scientific World Journal
Volume 2014, Article ID 476912, 8 pages
http://dx.doi.org/10.1155/2014/476912

Research Article

Observer Design for a Core Circadian Rhythm Network

Yuhuan Zhang

School of Mathematics and Information Sciences, Henan University, Kaifeng 475004, China

Correspondence should be addressed to Yuhuan Zhang; baiyigecun@163.com

Received 8 June 2014; Accepted 15 June 2014; Published 8 July 2014

Academic Editor: Guanghui Wen

The paper investigates the observer design for a core circadian rhythm network in *Drosophila* and *Neurospora*. Based on the constructed highly nonlinear differential equation model and the recently proposed graphical approach, we design a rather simple observer for the circadian rhythm oscillator, which can well track the state of the original system for various input signals. Numerical simulations show the effectiveness of the designed observer. Potential applications of the related investigations include the real-world control and experimental design of the related biological networks.

1. Introduction

Controllability, observability, and stability are typical problems of dynamical systems [1, 2]. Suppose we have a dynamical system with the following form:

$$\frac{dx}{dt} = f(t, x(t), u(t)), \tag{1}$$

where $x(t) \in R^N$ is the state vector of the system and $u(t) \in R^M$ is the input vector. System (1) is said to be observable, if we can find a function

$$y(t) = h(t, x(t), u(t)), \tag{2}$$

from which one can determine all the state variables of system (1). Here, $y(t) \in R^P$ depends on t, a set of the system's state $x(t)$ and the external input $u(t)$ [1–6].

For $f(t, x(t), u(t))$ with polynomial or rational expressions, existing results have reported that system (1) is observable if the Jacobian matrix $J = [J_{ij}]_{NP\times N}$ has full rank [3, 4], where J_{ij} is the Lie derivative of the output function $h(t, x(t), u(t))$.

Recently, Liu et al. [4] proposed a graphical approach to reduce the observability problem to a property of the inference diagram of a system. The inference diagram is based on the dynamical equation of the system. If x_j appears in x_i's differential equation, then there is a link from x_i to x_j in the inference diagram. The inference diagram can be decomposed into some strongly connected component (SCC). Those SCCs without incoming edges are called root SCCs. Liu et al. [4] reported that the number of the root SCCs provides the lower bound of the monitored state variables in $y(t)$. Furthermore, for many nonlinear systems, they declared that the number of the root SCCs provides not only necessary but also sufficient numbers of state variables to realize observability. That is, if the inference diagram of a system has k root SCCs, then one may only need to select k state variables from different root SCCs, and the system will be observable through monitoring these k state variables.

Biological systems are typical nonlinear systems [7–23]. Observer design for biological systems has important real-world implications. For example, through monitoring a few state variables of a complex biological system, if we can infer the state of the whole system, then lots of resources can be saved [4]. Circadian rhythms are typical biological phenomenon, which display endogenous, entrainable oscillations with a period that lasts approximately 24 hours. Circadian rhythms are widely in existence in various plants and animals [12], which are controlled by biomolecular networks. Circadian rhythms have been extensively investigated during the last decades [18–23]. For example, in 1995, Goldbeter established a mathematical model for the circadian rhythms in the *Drosophila* [11]. In 1999, Leloup et al. established a model for the circadian rhythms in the *Drosophila* and *Neurospora* [13]. In 2002, Gonze and coauthors [7] investigated the deterministic and stochastic dynamics in a core circadian

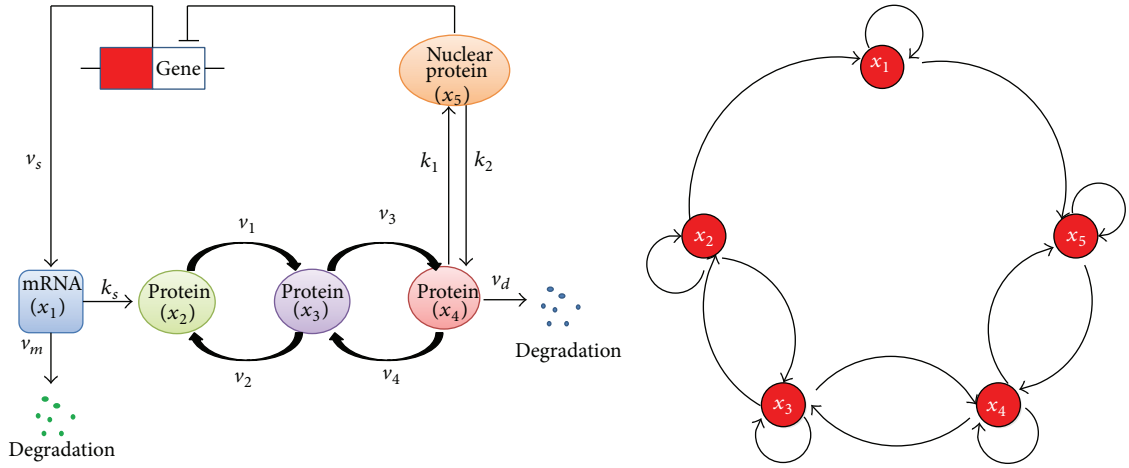

Figure 1: (a) A core model for circadian rhythms [7]. Parameters marked on the directed edges denote reaction rates. x_1 denotes the concentration of the mRNA; x_2, x_3, x_4, and x_5 are the concentrations of four forms of the protein expressed by the gene; x_2, x_3, and x_4 are cytosolic proteins; x_5 is nuclear protein. The circadian gene transcripts mRNA x_1 and then translates protein x_2. Proteins x_2, x_3, and x_4 can be reversibly phosphorylated successively. x_4 can be transported into the nucleus; the nucleus protein x_5 can negatively regulate the expression of the circadian gene. The mRNA and protein x_4 suffer from degradations. (b) The inference diagram [4] for the circadian rhythm model (3). If x_i appears in x_j's differential equation, then there will be a directed edge from x_j to x_i.

rhythm network. They found that the core network can display roughly the same circadian oscillations under both deterministic and stochastic descriptions.

In this paper, based on the graphical approach introduced by Liu et al. [4], for the core circadian rhythm network [7] in *Drosophila* and *Neurospora*, we design some simple observers for the network. Based on the Lyapunov stability theory, we theoretically verify the correctness of the designed observers. Finally, numerical simulations show the effectiveness of the designed observers for various input signals. The rest of the paper is organized as follows. In Section 2, we briefly introduce the mathematical model for the core circadian rhythm network. Observers will be designed in Section 3. We perform numerical simulations in Section 4. Discussions and some concluding remarks will be in Section 5.

2. The Core Circadian Rhythm Model

The core circadian rhythm network is reported by Gonze et al. [7]; the detailed biochemical processes are shown in Figure 1(a). Figure 1(a) represents a prototype for the molecular mechanism of circadian oscillations based on negative autoregulation of gene expression. Real-world circuits corresponding to Figure 1(a) include the *per* mRNA and *PER* protein in *Drosophila* [11, 12] and *frq* mRNA and *FRQ* protein in *Neurospora* [13].

The core model involves gene transcription and transport of mRNA x_1 into the cytosol where it is translated into protein x_2 and degraded. Protein x_2 can be reversibly phosphorylated from the form x_2 into the forms x_3 and x_4, successively. The phosphorylated protein x_4 is degraded or transported into the nucleus, and the nucleus protein x_5 can negatively regulate the expression of its gene. Based on the work from Gonze et al. [7] in 2002, the modified mathematical model

Table 1: Parameter values.

Parameter	Value
v_s	0.5 nMh^{-1}
n	4
K_m	0.2 nM
v_1	6.0 nMh^{-1}
v_2	3.0 nMh^{-1}
v_3	6.0 nMh^{-1}
v_4	3.0 nMh^{-1}
v_d	1.5 nMh^{-1}
k_1	2.0 h^{-1}
K_I	2 nM
v_m	0.3 nMh^{-1}
k_s	2.0 h^{-1}
K_1	1.5 nM
K_2	2.0 nM
K_3	1.5 nM
K_4	2.0 nM
K_d	0.1 nM
k_2	1.0 h^{-1}

for the core circadian model can be established as follows. Consider

$$\frac{dx_1}{dt} = v_s \frac{K_I^n}{K_I^n + x_5^n} - v_m \frac{x_1}{K_m + x_1} + u(t),$$

$$\frac{dx_2}{dt} = k_s x_1 - v_1 \frac{x_2}{K_1 + x_2} + v_2 \frac{x_3}{K_2 + x_3},$$

$$\begin{aligned}
\frac{dx_3}{dt} &= v_1\frac{x_2}{K_1+x_2} - v_2\frac{x_3}{K_2+x_3} - v_3\frac{x_3}{K_3+x_3} + v_4\frac{x_4}{K_4+x_4},\\
\frac{dx_4}{dt} &= v_3\frac{x_3}{K_3+x_3} - v_4\frac{x_4}{K_4+x_4} - v_d\frac{x_4}{K_d+x_4} - k_1x_4 + k_2x_5,\\
\frac{dx_5}{dt} &= k_1x_4 - k_2x_5,
\end{aligned} \tag{3}$$

where x_i $(i = 1, \ldots, 5)$ are state variables, which correspond to species concentrations of the mRNA, the four forms of proteins. $u(t)$ represents the external input, which can be seen as the effect of the environment on the system. K_i $(i = I, m, 1, 2, 3, 4, d)$, k_j $(j = 1, 2, s)$, and v_k $(k = s, m, 1, 2, 3, 4, d)$ are Michaelis constants, first-order reaction rate constants, and maximum rates of protein degradation, transcription, and phosphorylation. It is noted that if we set $u(t) = 0$, then system (3) degenerates into the model investigated in [7]. A typical set of parameter values for system (3) are shown in Table 1. Under the parameter values as shown in Table 1 and for $u(t) = 0$, dynamical system (3) can display circadian rhythms with a period close to 24 hours.

3. Observer Design for the Circadian Rhythm Model

For simplicity, in the following, we rewrite system (3) as the following form:

$$\begin{aligned}
\frac{dx}{dt} &= Ax(t) + f(x(t), u(t)),\\
y(t) &= Cx(t),
\end{aligned} \tag{4}$$

where $x(t) = (x_1(t), \ldots, x_5(t))^T$ and $f(x(t), u(t)) \in R^5$ denotes the nonlinear term. $y(t)$ denotes the monitored output. C is a constant matrix. $Ax(t)$ denotes the linear term, with

$$A = \begin{bmatrix} 0 & 0 & 0 & 0 & 0\\ k_s & 0 & 0 & 0 & 0\\ 0 & 0 & 0 & 0 & 0\\ 0 & -k_1 & 0 & 0 & k_2\\ 0 & k_1 & 0 & 0 & -k_2 \end{bmatrix}. \tag{5}$$

For system (4), similar to the works in [4–6], our objective is to design the following observer, which can track the states of system (4):

$$\frac{dz}{dt} = Az(t) + f(z(t), u(t)) + K(y(t) - Cz(t)), \tag{6}$$

where K is a gain matrix, which is to be determined. The estimation error dynamics are then given by

$$\frac{de}{dt} = (A - KC)e(t) + [f(x(t), u(t)) - f(z(t), u(t))], \tag{7}$$

where $e(t) = x(t) - z(t)$.

From Liu et al. [4], the observability of a dynamical system can be revealed by its inference diagram. The inference diagram of system (3) is shown in Figure 1(b), where the five nodes are strongly connected and consist of the single root SCC. From the conclusion in [4], system (3) is observable, and one should only monitor any one of the five nodes in Figure 1(b). In the following, for simplicity, we assume that only $x_1(t)$ is monitored. The designed observer of system (3) is described as

$$\begin{aligned}
\frac{dz_1}{dt} &= v_s\frac{K_I^n}{K_I^n + z_5^n} - v_m\frac{z_1}{K_m + z_1} + u(t) + kc(x_1 - z_1),\\
\frac{dz_2}{dt} &= k_sz_1 - v_1\frac{z_2}{K_1 + z_2} + v_2\frac{z_3}{K_2 + z_3},\\
\frac{dz_3}{dt} &= v_1\frac{z_2}{K_1 + z_2} - v_2\frac{z_3}{K_2 + z_3} - v_3\frac{z_3}{K_3 + z_3} + v_4\frac{z_4}{K_4 + z_4},\\
\frac{dz_4}{dt} &= v_3\frac{z_3}{K_3 + z_3} - v_4\frac{z_4}{K_4 + z_4} - v_d\frac{z_4}{K_d + z_4} - k_1z_4 + k_2z_5,\\
\frac{dx_5}{dt} &= k_1z_4 - k_2z_5,
\end{aligned} \tag{8}$$

where k, c are the nonzero elements in matrix K and C of (6). For simplicity, we denote

$$g(K_j, x_i) = \frac{x_i}{K_j + x_i}. \tag{9}$$

Then,

$$\frac{K_I^n}{K_I^n + x_5^n} = 1 - g(K_I^n, x_5^n). \tag{10}$$

The corresponding error dynamics are described as

$$\begin{aligned}
\frac{de_1}{dt} &= v_s[g(K_I^n, z_5^n) - g(K_I^n, x_5^n)]\\
&\quad - v_m[g(K_m, x_1) - g(K_m, z_1)] - kce_1,\\
\frac{de_2}{dt} &= k_se_1 - v_1[g(K_1, x_2) - g(K_1, z_2)]\\
&\quad + v_2[g(K_2, x_3) - g(K_2, z_3)],\\
\frac{de_3}{dt} &= v_1[g(K_1, x_2) - g(K_1, z_2)]\\
&\quad - v_2[g(K_2, x_3) - g(K_2, z_3)]\\
&\quad - v_3[g(K_3, x_3) - g(K_3, z_3)]\\
&\quad + v_4[g(K_4, x_4) - g(K_4, z_4)],\\
\frac{de_4}{dt} &= v_3[g(K_3, x_3) - g(K_3, z_3)]\\
&\quad - v_4[g(K_4, x_4) - g(K_4, z_4)]\\
&\quad - v_d[g(K_d, x_4) - g(K_d, z_4)] - k_1e_4 + k_2e_5,\\
\frac{de_5}{dt} &= k_1e_4 - k_2e_5.
\end{aligned} \tag{11}$$

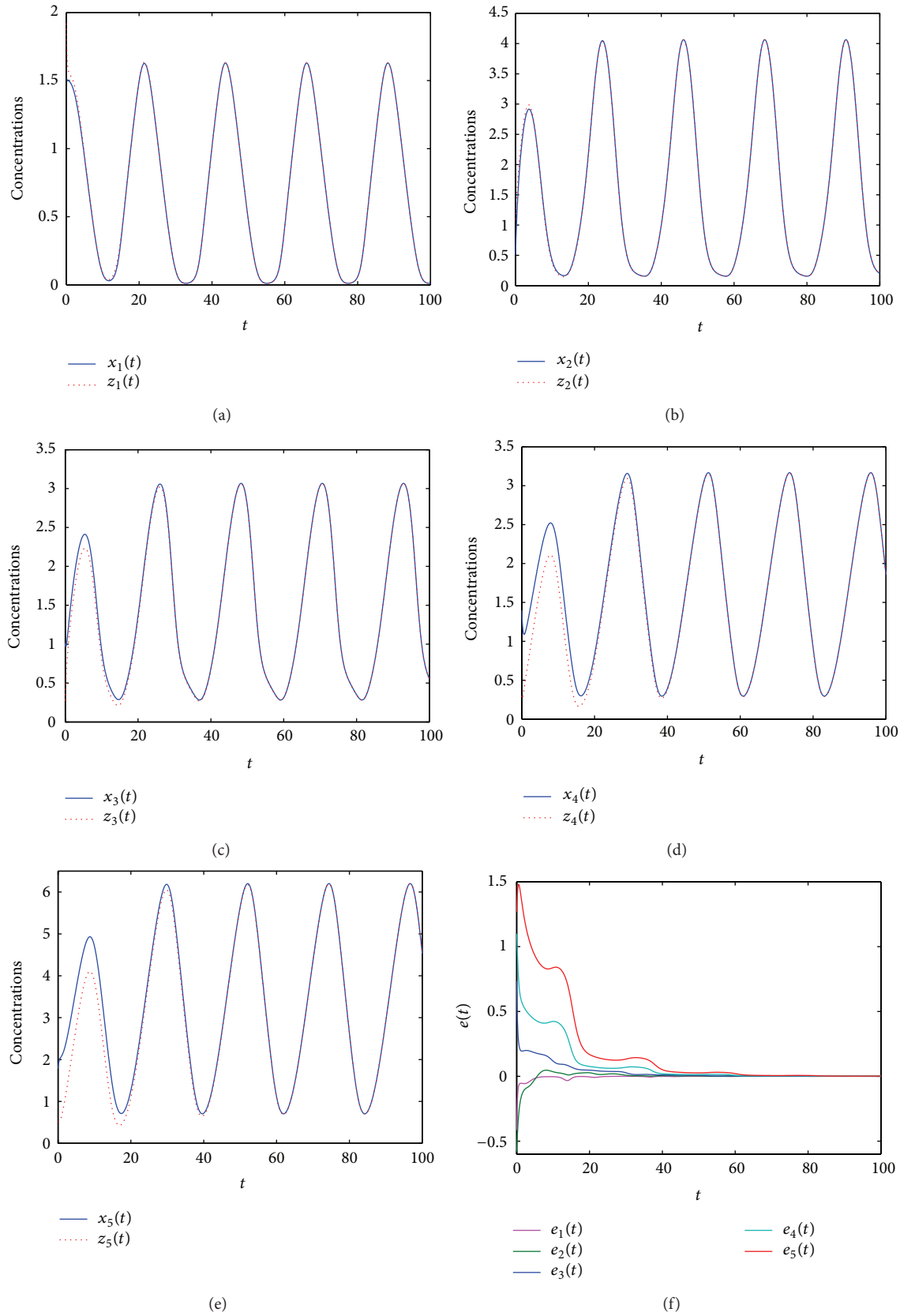

FIGURE 2: (a)–(e) State trajectories of systems (3) and (8). (f) The error dynamics of system (11). Here, $u(t) = 0$, $y(t) = x_1(t)$, and $k = 5$. Initial values are randomly chosen.

Before we analyze the stability of system (11), we note that since x_i, z_i represent species concentrations, they must be nonnegative and bounded [24]. Furthermore, since $g(K_j, x_i)$ is continuous and differentiable, by the mean value theorem, there must exist ξ_i between x_i and z_i, satisfying

$$g\left(K_j, x_i\right) - g\left(K_j, z_i\right) = g'\left(K_j, \xi\right)\left(x_i - z_i\right) = \frac{K_j}{\left(K_j + \xi_i\right)^2}\left(x_i - z_i\right). \tag{12}$$

For system (11), we construct the following Lyapunov function:

$$V(t) = \frac{1}{2}\sum_{i=1}^{5} e_i(t)^2. \tag{13}$$

Based on (12), the derivative of (13) along system (11) is

$$\begin{aligned}\dot{V}(t) &= \sum_{i=1}^{5} e_i(t)\,\dot{e}_i(t)\\ &= -\left[kc + \frac{V_m K_m}{\left(K_m + \xi_1\right)^2}\right]e_1^2 - \frac{V_1 K_1}{\left(K_1 + \xi_2\right)^2}e_2^2\\ &\quad - \left[\frac{V_2 K_2}{\left(K_2 + \xi_3\right)^2} + \frac{V_3 K_3}{\left(K_3 + \xi_3'\right)^2}\right]e_3^2\\ &\quad - \left[\frac{V_4 K_4}{\left(K_4 + \xi_4\right)^2} + \frac{V_d K_d}{\left(K_d + \xi_4'\right)^2} + k_1\right]e_4^2\\ &\quad - k_2 e_5^2 + k_s e_1 e_2 + \left[\frac{V_2 K_2}{\left(K_2 + \xi_3\right)^2} + \frac{V_1 K_1}{\left(K_1 + \xi_2\right)^2}\right]e_2 e_3\\ &\quad + \left(k_1 + k_2\right)e_4 e_5\\ &\quad + \left[\frac{V_4 K_4}{\left(K_4 + \xi_4\right)^2} + \frac{V_3 K_3}{\left(K_3 + \xi_3'\right)^2}\right]e_3 e_4 - \frac{n V_s K_I^n \xi_5^{n-1}}{\left(K_I^n + \xi_5^n\right)^2}e_1 e_5\\ &= e^T Q e.\end{aligned} \tag{14}$$

Here,

$$Q = \begin{bmatrix} \frac{-V_m K_m}{\left(K_m + \xi_1\right)^2} - kc & \frac{k_s}{2} & 0 & 0 & \frac{-n V_s K_I^n \xi_5^{n-1}}{2\left(K_I^n + \xi_5^n\right)^2}\\ * & \frac{-V_1 K_1}{\left(K_1 + \xi_2\right)^2} & \frac{0.5 V_2 K_2}{\left(K_2 + \xi_3\right)^2} + \frac{0.5 V_1 K_1}{\left(K_1 + \xi_2\right)^2} & 0 & 0\\ 0 & * & \frac{-V_2 K_2}{\left(K_2 + \xi_3\right)^2} - \frac{V_3 K_3}{\left(K_3 + \xi_3'\right)^2} & \frac{0.5 V_4 K_4}{\left(K_4 + \xi_4\right)^2} + \frac{0.5 V_3 K_3}{\left(K_3 + \xi_3'\right)^2} & 0\\ 0 & 0 & * & \frac{-V_4 K_4}{\left(K_4 + \xi_4\right)^2} - \frac{V_d K_d}{\left(K_d + \xi_4'\right)^2} - k_1 & \frac{k_1 + k_2}{2}\\ * & 0 & 0 & * & -k_2 \end{bmatrix}, \tag{15}$$

which is a symmetrical matrix. ξ_i, ξ_i' are values between x_i and z_i. For appropriate gain k, if $Q < 0$, $\dot{V}(t) < 0$. System (11) will be globally asymptotically stable. In other words, system (3) can be observed through the observer (8).

Remark 1. If any one of the other variables is used to track the state of the original system (3), one should only slightly revise the observer (8). If more than one variable is measured to track the original system, the observer can be similarly designed. For example, if $y(t)$ in (4) is $y(t) = (c_1 x_1, c_2 x_2)^T$, the control gain matrix K is chosen as

$$K = \begin{bmatrix} \alpha & 0\\ 0 & \beta\\ 0 & 0\\ 0 & 0\\ 0 & 0 \end{bmatrix}. \tag{16}$$

Then, the observer is designed as

$$\begin{aligned}\frac{dz_1}{dt} &= v_s\frac{K_I^n}{K_I^n + z_5^n} - v_m\frac{z_1}{K_m + z_1} + u(t) + \alpha c_1\left(x_1 - z_1\right),\\ \frac{dz_2}{dt} &= k_s z_1 - v_1\frac{z_2}{K_1 + z_2} + v_2\frac{z_3}{K_2 + z_3} + \beta c_2\left(x_2 - z_2\right),\\ \frac{dz_3}{dt} &= v_1\frac{z_2}{K_1 + z_2} - v_2\frac{z_3}{K_2 + z_3} - v_3\frac{z_3}{K_3 + z_3} + v_4\frac{z_4}{K_4 + z_4},\\ \frac{dz_4}{dt} &= v_3\frac{z_3}{K_3 + z_3} - v_4\frac{z_4}{K_4 + z_4} - v_d\frac{z_4}{K_d + z_4} - k_1 z_4 + k_2 z_5,\\ \frac{dx_5}{dt} &= k_1 z_4 - k_2 z_5.\end{aligned} \tag{17}$$

For appropriate parameters α, β, one can easily prove that the original system is also observable from the observer (17).

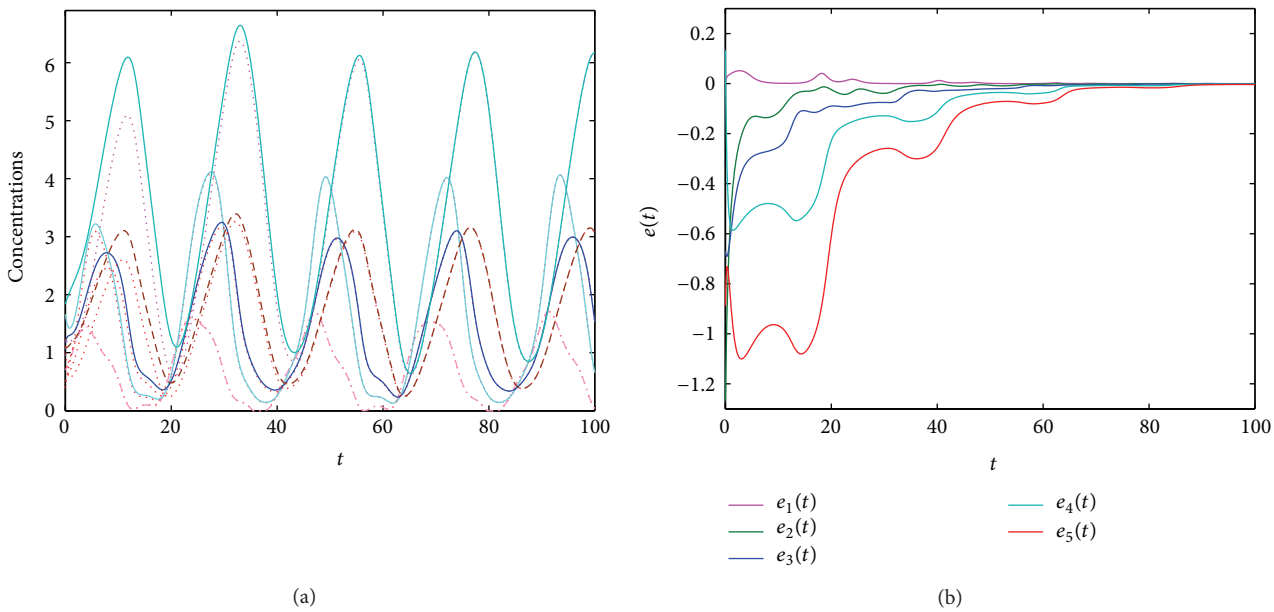

(a) (b)

FIGURE 3: (a) State trajectories of systems (3) and (8) with $u(t) = \epsilon \sin(t)$. (b) The error dynamics of system (11). Here, $y(t) = cx_1(t)$, $k = 2.5$, $c = 2$, and $\epsilon = 0.1$.

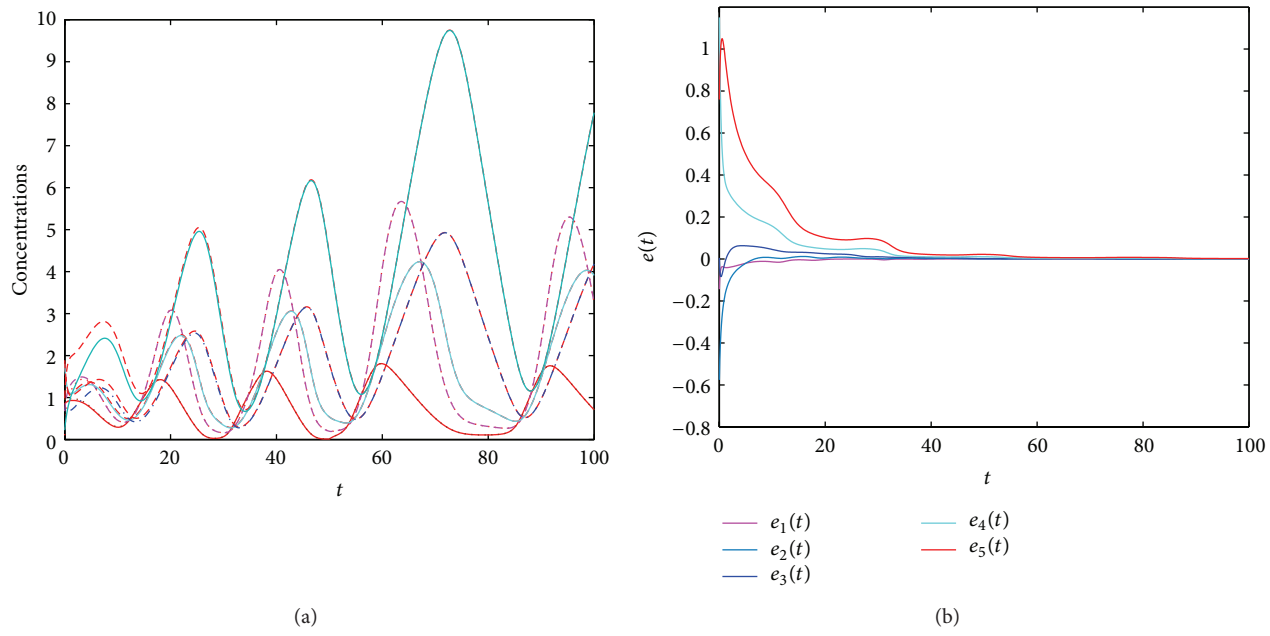

(a) (b)

FIGURE 4: (a) State trajectories of systems (3) and (8) with step input signal $u(t)$. (b) The error dynamics of system (11). Here, $y(t) = cx_1(t)$, $k = 2.5, c = 2$, and $u(t) = 0$ for $t \leq 50$ and $u(t) = 0.1$ for $t > 50$.

Obviously, the corresponding observer (17) is more complex than the observer (11).

Remark 2. There are many methods to prove the stability of a dynamical system. One can easily prove that the nonlinear terms on the right-hand side of system (11) are Lipschitz. For Lipschitz nonlinear systems, Rajamani [5] proposed a general theorem for the observer design. However, due to the complexity of the biological model, the theorem obtained in [5] fails to work for the error system (11). Therefore, we have used the mean value theorem to simplify the error system (11) and obtained a sufficient condition for the observer design. The matrix Q relies on the bound of system (3).

4. Numerical Simulations

Hereinafter, we numerically verify the effectiveness of the designed observers. Firstly, we assume $u(t) = 0$; the output

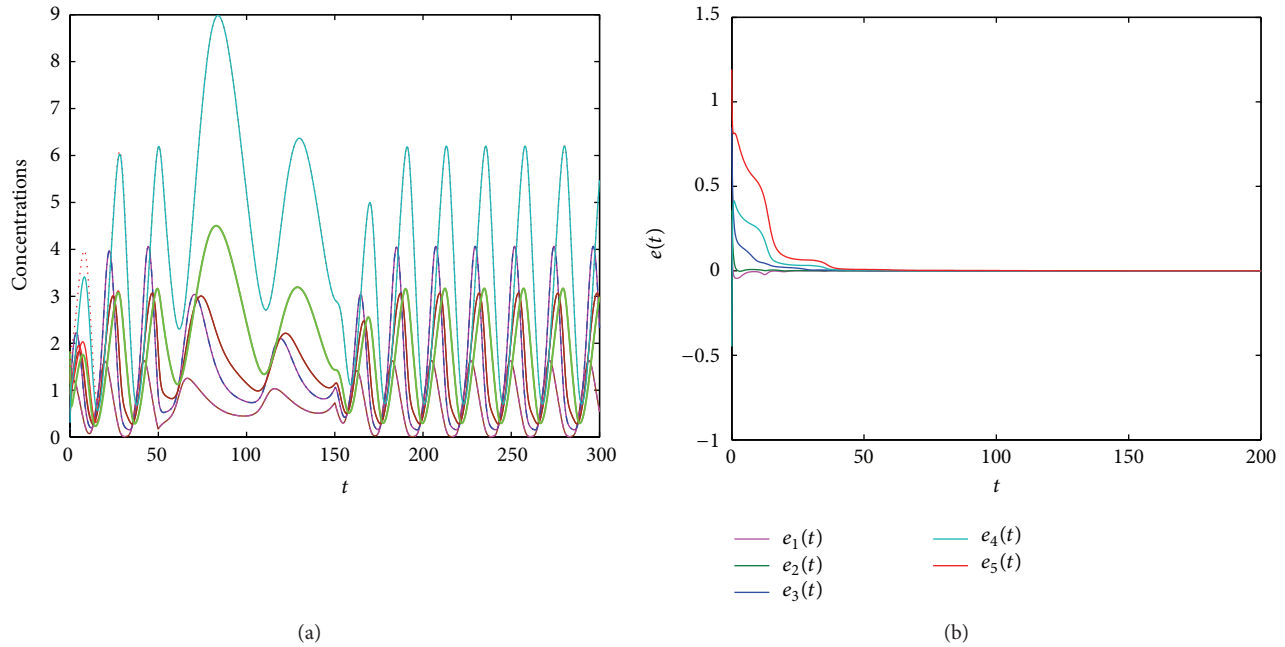

(a) (b)

FIGURE 5: (a) State trajectories of systems (3) and (17) with step input signal $u(t)$ in (19). (b) The error dynamics between systems (3) and (17). Here $y(t) = (c_1x_1(t), c_2x_2(t))^T$, $\alpha = 2$, $\beta = 3$, $c_1 = 2.2$, and $c_2 = 1$.

function $y(t) = x_1(t)$. For $k = 5$, all the state variables in the original system (3) can be tracked by the observer (8). Under randomly initial values, Figure 2 shows the state trajectories of systems (3) and (8), as well as the error dynamics of system (11). From Figure 2, one can see that the state variables of (3) oscillate with a period close to 24 hours. The observer system (8) can track the states of the original system. The error between the observer system and the original system quickly approximates to zero.

For different input signals and under appropriate gain k, system (8) can always track the states of system (3). For example, when $u(t) = \epsilon \sin(t)$, $y(t) = cx_1(t), k = 2.5, c = 2$, and $\epsilon = 0.1$, Figure 3 shows the state trajectories of systems (3) and (8) as well as the error dynamics of system (11). From Figure 3, we can see that the states of system (3) can be observed by the observer (8). The error system (11) converges to zero quickly. When $u(t)$ is a step signal, the observer (11) can also well monitor the states of the original (3). Figure 4 shows the case for $y(t) = cx_1(t)$, $k = 2.5$, and $c = 2$, and the step input signal

$$u(t) = \begin{cases} 0, & t \le 50, \\ 0.1, & t > 50. \end{cases} \tag{18}$$

For the cases discussed in Remark 1, when we choose $\alpha = 2$, $\beta = 3$, $c_1 = 2.2$, $c_2 = 1$, and the following input signal,

$$u(t) = \begin{cases} 0, & t \le 50, \\ 0.2, & 50 < t < 150, \\ 0, & t \ge 150, \end{cases} \tag{19}$$

Figure 5 shows the numerical simulation results for such case. From Figure 5, we see that the observer (17) can also well track the states of system (3). Additionally, combined with the simulation results as shown in Figures 2–5, we can conclude that the designed observers have good performance under various kinds of inputs, and the input signal $u(t)$ can affect the period of the circadian oscillator.

5. Discussions and Conclusions

Biological systems are typical complex dynamical systems. To efficiently infer the state of a biological system, it is necessary to develop some simple observers via monitoring a few system variables. Based on the recently proposed graphical approach, we have designed some rather simple observers for a core circadian rhythm network. For various input signals and under appropriate control gains, the designed observer can well infer the states of the original system. The investigations in this paper further support the conclusions in [4]. Real-world applications of the related investigations on biological networks include the experimental design and control of the related biological systems.

We have considered three types of inputs, and it is intriguing to investigate the observer design problems for stochastic systems, since biological systems are inherent stochastic and perturbed by environment [14–16]. Another question that deserves to be further investigated is to develop some general theorems to guarantee the observability of the biological systems [25–28]. Finally, it is also intriguing to investigate the observability of large-scale biological networks [17], such as the yeast cell cycle network with boolean dynamical model or differential equation models [18–23]. These topics will be discussed in our future works.

Conflict of Interests

The authors declare that there is no conflict of interests regarding the publication of this paper.

Acknowledgments

This work was supported by the National Natural Science Foundation of China under Grant no. 61304151 and the Science Foundation of Henan University under Grants nos. 2012YBZR007 and 2013YBRW005.

References

[1] B. C. Moore, "Principal component analysis in linear systems: controllability, observability, and model reduction," *IEEE Transactions on Automatic Control*, vol. 26, no. 1, pp. 17–32, 1981.

[2] J. P. Gauthier and I. Kupka, *Deterministic Observation Theory and Applications*, Cambridge University Press, 2001.

[3] S. Diop and M. Fliess, "Nonlinear observability, identifiability, and persistent trajectories," in *Proceedings of the 30th IEEE Conference on Decision and Control*, vol. 1, pp. 714–719, December 1991.

[4] Y.-Y. Liu, J.-J. Slotine, and A.-L. Barabási, "Observability of complex systems," *Proceedings of the National Academy of Sciences of the United States of America*, vol. 110, no. 7, pp. 2460–2465, 2013.

[5] R. Rajamani, "Observers for Lipschitz nonlinear systems," *IEEE Transactions on Automatic Control*, vol. 43, no. 3, pp. 397–401, 1998.

[6] J. Tsinias, "Observer design for nonlinear systems," *Systems and Control Letters*, vol. 13, no. 2, pp. 135–142, 1989.

[7] D. Gonze, J. Halloy, and A. Goldbeter, "Deterministic versus stochastic models for circadian rhythms," *Journal of Biological Physics*, vol. 28, no. 4, pp. 637–653, 2002.

[8] P. Wang, X. Yu, and J. Lü, "Identification and evolution of structurally dominant nodes in protein protein interaction networks," *IEEE Transactions on Biomedical Circuits and Systems*, vol. 8, no. 1, pp. 87–97, 2014.

[9] P. Wang and J. Lü, "Control of genetic regulatory networks: opportunities and challenges," *Acta Automatica Sinica*, vol. 39, no. 12, pp. 1969–1979, 2013.

[10] P. Wang, J. Lü, and M. J. Ogorzalek, "Global relative parameter sensitivities of the feed-forward loops in genetic networks," *Neurocomputing*, vol. 78, no. 1, pp. 155–165, 2012.

[11] A. Goldbeter, "A model for circadian oscillations in the Drosophila period protein (PER)," *Proceedings of the Royal Society B: Biological Sciences*, vol. 261, no. 1362, pp. 319–324, 1995.

[12] A. Goldbeter, *Biochemical Oscillations and Cellular Rhythms. The Molecular Bases of Periodic and Chaotic Behaviour*, Cambridge University Press, Cambridge, UK, 1996.

[13] J. Leloup, D. Gonze, and A. Goldbeter, "Limit cycle models for circadian rhythms based on transcriptional regulation in *Drosophila* and *Neurospora*," *Journal of Biological Rhythms*, vol. 14, no. 6, pp. 433–448, 1999.

[14] L. Wan, Q. Zhou, Z. Zhou, and P. Wang, "Dynamical behaviors of the stochastic Hopfield neural networks with mixed time delays," *Abstract and Applied Analysis*, vol. 2013, Article ID 384981, 8 pages, 2013.

[15] S. Wang, Y. Shen, C. Shi, T. Wang, Z. Wei, and H. Li, "Defining biological networks for noise buffering and signaling sensitivity using approximate Bayesian computation," *The Scientific World Journal*, vol. 2014, Article ID 625754, 12 pages, 2014.

[16] P. Wang, J. Lü, L. Wan, and Y. Chen, "A stochastic simulation algorithm for biochemical reactions with delays," in *Proceedings of the IEEE International Conference on Systems Biology*, pp. 109–114, Huangshan, China, August 2013.

[17] P. Wang, R. Lu, Y. Chen, and X. Wu, "Hybrid modelling of the general middle-sized genetic regulatory networks," in *Proceedings of the IEEE International Symposium on Circuits and Systems (ISCAS '13)*, pp. 2103–2106, Beijing, China, May 2013.

[18] B. Novak and J. J. Tyson, "Modeling the control of DNA replication in fission yeast," *Proceedings of the National Academy of Sciences of the United States of America*, vol. 94, no. 17, pp. 9147–9152, 1997.

[19] A. Sveiczer, J. J. Tyson, and B. Novak, "Modelling the fission yeast cell cycle," *Briefings in Functional Genomics and Proteomics*, vol. 2, no. 4, pp. 298–307, 2004.

[20] F. Li, T. Long, Y. Lu, Q. Ouyang, and C. Tang, "The yeast cell-cycle network is robustly designed," *Proceedings of the National Academy of Sciences of the United States of America*, vol. 101, no. 14, pp. 4781–4786, 2004.

[21] B. Novak, Z. Pataki, A. Ciliberto, and J. J. Tyson, "Mathematical model of the cell division cycle of fission yeast," *Chaos*, vol. 11, no. 1, pp. 277–286, 2001.

[22] B. Novak and J. J. Tyson, "Quantitative analysis of a molecular model of mitotic control in fission yeast," *Journal of Theoretical Biology*, vol. 173, no. 3, pp. 283–305, 1995.

[23] B. Novak, K. C. Chen, and J. J. Tyson, "Systems biology of the yeast cell cycle engine," in *Systems Biology: Definitions and Perspectives*, L. Alberghina and H. V. Westerhoff, Eds., vol. 13 of *Topics in Current Genetics*, pp. 305–324, Springer, Berlin, Germany, 2005.

[24] P. Wang, D. Li, X. Wu, and J. Lü, "Ultimate bound estimation of a class of high dimensional quadratic autonomous dynamical systems," *International Journal of Bifurcation and Chaos*, vol. 21, no. 9, pp. 2679–2694, 2011.

[25] G. Wen, Z. Duan, G. Chen, and W. Yu, "Consensus tracking of multi-agent systems with Lipschitz-type node dynamics and switching topologies," *IEEE Transactions on Circuits and Systems I: Regular Papers*, vol. 61, no. 2, pp. 499–511, 2014.

[26] J. Qiu and J. Cao, "Global synchronization of delay-coupled genetic oscillators," *Neurocomputing*, vol. 72, no. 16–18, pp. 3845–3850, 2009.

[27] T. Zhou, J. Zhang, Z. Yuan, and L. Chen, "Synchronization of genetic oscillators," *Chaos*, vol. 18, no. 3, Article ID 037126, 2008.

[28] G. Wen, W. Yu, Y. Zhao, and J. Cao, "Pinning synchronisation in fixed and switching directed networks of Lorenz-type nodes," *IET Control Theory & Applications*, vol. 7, no. 10, pp. 1387–1397, 2013.